

Dissipative structures produced by supersonic motion of domain walls in orthoferrites

M. V. Chetkov, A. K. Zvezdin, S. N. Gadetskii, S. V. Gomovon, V. B. Smirnov, and Yu. N. Kurbatova

Moscow State University

(Submitted 28 May 1987)

Zh. Eksp. Teor. Fiz. **94**, 269–279 (January 1988)

It is shown theoretically and experimentally that periodic structures are produced in domain walls moving at supersonic velocity. These structures are the result of the balance of surface, tension, and dissipative forces applied by an external magnetic field. A feature of the structures on a moving domain wall is the presence of singularities of the “cusp” type. With increase of H , the period λ of the structures decreases and tends under the experimental conditions to $\lambda = 250 \mu\text{m}$. The structures are stationary in magnetic fields that are not much stronger than the field at which the sound barrier is crossed. The value of λ does not vary as the wall moves, and the amplitude of the structures relaxes towards smaller values faster, the larger the H . It is shown that similar structures are realized also on iron-garnet film domain walls.

1. INTRODUCTION

The maximum speed of domain walls (DW) in orthoferrites exceeds substantially the speed of sound.¹ We demonstrate in the present paper that periodic non-one-dimensional structures are produced on a DW in the course of a transition to supersonic motion. These structures are generated at the location of the negative differential mobility produced by the action of a dissipative force of magnetoelastic origin. The structure formation is more pronounced the higher the DW mobility. It is important that the effect takes place in a homogeneous medium and in an external field that is uniform in the DW plane, so that one can speak of self-organization of the system.²

The formation of a structure on an immobile DW is usually attributed to its magnetostatic interaction with magnetic poles on the surface of the sample and on the wall itself. It is known that a planar DW is unstable to flexural perturbations. It can be stabilized with the aid, e.g., of a non-uniform external magnetic field with sufficiently large gradient H'_z , where z is the direction of the easy-magnetization axis. Such a gradient can be produced artificially for an isolated DW in the investigated sample. It always exists in a stripe-domain structure and is determined by the demagnetizing fields of the neighboring domains. Hagedorn³ has shown that if the easy-magnetization axis is perpendicular to the sample plane, the requirement for DW stability is that the field gradient exceed a certain critical value (on the order of 10^3 Oe/cm for YFeO_3). When the field gradient drops below a critical value, the DW is bent and acquires a structure whose period is determined by the magnetostatic interaction.

We show in the present paper that in the case of a moving DW there exists a fundamentally different mechanism which also produces periodic structures on the wall. This mechanism is connected with dissipation of the energy of the moving DW and can be of basic importance of materials with low saturation magnetization, e.g., for weak ferromagnets. Besides dissipation, a DW moving with supersonic velocity is subject to instability of the planar front and to strongly pronounced nonlinearity, which are known necessary conditions for self-organization.² Particular interest at-

taches to the presence on the DW of “cusp” singularities (see Fig. 2), i.e., discontinuities of the spatial derivative of the coordinate of the center of the DW.

2. EXPERIMENT

The dynamics of domain walls and dissipative structure produced on them on passing through the speed of sound was investigated at a temperature 300 K for chemically polished yttrium-orthoferrite plates $100 \mu\text{m}$ thick and cut perpendicular to the optical axis. A stable isolated domain wall was obtained in a gradient 300 Oe/cm . The magnetic field was produced on the sample surface by attaching a pair of coils of 1.5 mm diameter and of nine turns each, thus ensuring a magnetic-field pulse rise time 6–8 ns.

The dissipative structures on the domains walls were investigated by twofold high-speed photography.⁴ The high DW speeds (up to 20 km/s) restrict the duration of the light pulse. To obtain pulses shorter than 1 ns we constructed a system of two TEA lasers, a generator and an amplifier (Fig. 1). The amplifier increases substantially the radiation power and decreases the light-beam divergence. The generator and amplifier are arranged in tandem and have a common grounded base plate. The generator and amplifier laser channels were respectively 10 and 25 cm long. The charging plates were triangular and made contact through one of the discharge-gap electrodes. The Blumlein line was made from five or six sheets of aluminum foil separated by teflon films having $\epsilon = 4$ and a thickness $25 \mu\text{m}$. This made it easy to change the shape and dimensions of the plates, and thus control the duration and energy of the output pulse. The system had a common trigatron-type discharge unit operating at frequencies up to 10 Hz. The generator was synchronized with the amplifier by varying the distance between their electrodes. The optimal distance d between the electrodes at a supply voltage $+10 \text{ kV}$ was 2–3 mm for the generator and 3 mm for the amplifier.

The geometric dimensions of the plates were chosen to produce a “traveling wave” not only in the generator but also in the amplifier; this shortened light pulse substantially. After pumping the dye (oxazine), the light-pulse duration was 200 ps, as against 800 ps for a single TEA laser with a

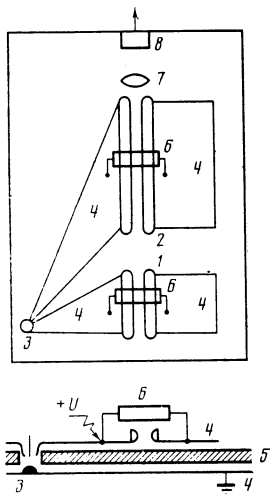


FIG. 1. Diagram of nitrogen TEA-TEA laser: 1— generator electrodes; 2— amplifier electrodes; 3— spark-gap discharge unit; 4— charging plates; 5— dielectric; 6— resistor; 7— converging lens; 8— dye-filled cell.

laser-channel length 25 cm. The output pulse energy was 8 μJ at a wavelength $\lambda = 0.36 \mu\text{m}$. The light-pulse parameters were measured with an "Agat" SF-1 camera. The light intensity, the large Faraday rotation, and the transparency of the yttrium orthoferrite made it possible to record the instantaneous positions of the dynamic domain structure directly on sensitive photographic film without the use of a brightness amplifier.

The light beam was split by a mirror into two. The second beam was delayed relative to the first by a mirror system. The direct and delayed light pulses passed through separate polarizers, were incident on the sample, and proceeded next through a common analyzer to the photographic-recording system. The region covered by the DW between two light pulses is shown as a dark strip against a light background (Fig. 2).

3. EXPERIMENTAL RESULTS

It was shown in Ref. 5 that a DW becomes unstable on going through the sound barrier, and non-one-dimensional leading sections are produced on it. These sections are more developed the larger the value of $\mu\Delta H/s$ (Ref. 6). Here μ is the DW mobility, ΔH the width of the region of constant velocity of the DW on the $v(H)$ plot for a DW at the speed of sound s . Theoretical calculations of ΔH were carried out in Refs. 7 and 8. In our present experiments we have observed that these inhomogeneities in homogeneous samples and in a magnetic field that is uniform along the DW are strictly periodic. Figure 2 shows several twofold high-speed photographs of the dynamic domain structure in a YFeO_3 plate. At 300 K the DW mobility was $10^4 \text{ cm/s}\cdot\text{Oe}$. The dark strip is the region negotiated by the DW during the time between two light pulses. Attention is called to the spatial periodicity of the DW moving with supersonic velocity. Note the singularities on the moving DW, where the derivative of the displacement with respect to the coordinate becomes discontinuous. Figure 2a shows how weak periodic bends, patently nonsinusoidal in shape, are formed on a straight DW and develop with time and occupy gradually the entire DW.

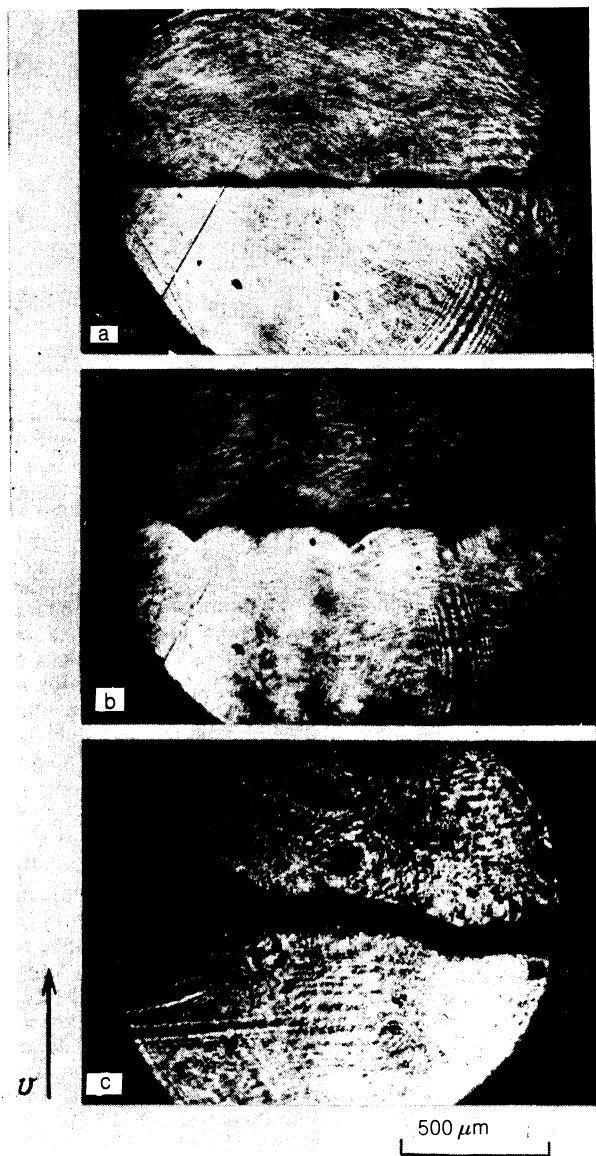


FIG. 2. Twofold high-speed photographs of structures on a dynamic domain wall in YFeO_3 in a field H and at delays Δt . Dark strip—region traversed by the DW in the time Δt : a— $H = 1000 \text{ Oe}$, $\Delta t = 2 \text{ ns}$; b— $H = 1000 \text{ Oe}$, $\Delta t = 2 \text{ ns}$; c— $H = 150 \text{ Oe}$, $\Delta t = 8 \text{ ns}$.

It is seen on the photographs of Fig. 2 and on similar ones that the boundary conditions produced by the coils on the edges of the DW do not influence the structure produced on the DW on going through the sound barrier. The period of the structure depends on the magnetic field (Fig. 3). In our experiment it decreased with increase of H , first rapidly and then more slowly—from 1200 to $250 \mu\text{m}$. In all our experiments the period of the structure tended, with increase of H , to the same value $\lambda = 250 \mu\text{m}$, which is the limiting value of the period of the structure.

Figure 4 shows a sequence of high-speed photographs of a moving DW, taken in the DW contrast regime at supersonic velocity. It shows a distinct periodic structure. At the instant of passage through the sound barrier the DW broadens to $25 \mu\text{m}$ (Fig. 4a). This is much larger than its displacement in a time equal to the duration of the light pulse, and

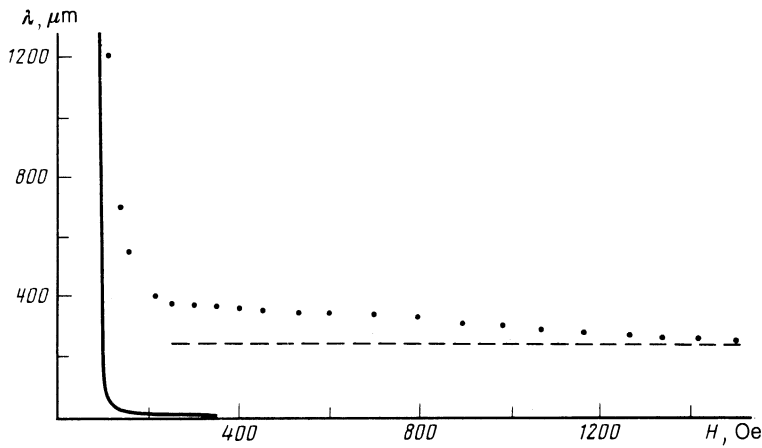


FIG. 3. Experimental (points) and theoretical [solid curve—according to (9), dashed—according to (11)] plots of the period of the dissipative structure vs the pulsed magnetic field H .

approximately half the value previously reported for a light pulse duration 2 ns (Ref. 4). This is evidence that the DW is tilted in the sample plane on going through the sound barrier. As it moves on, the DW straightens out and its width decreases (Fig. 4b). These photographs show that the period of the dynamic structure does not change with time. The structure amplitude first increases so long as there are linear sections on the DW. The amplitude is a maximum at the instant when neighboring non-one-dimensional formation collapse. This is precisely the instant when the singularities on the DW are most pronounced. The structure amplitude begins then to relax, with the relaxation rate strongly dependent on the period of the structure.

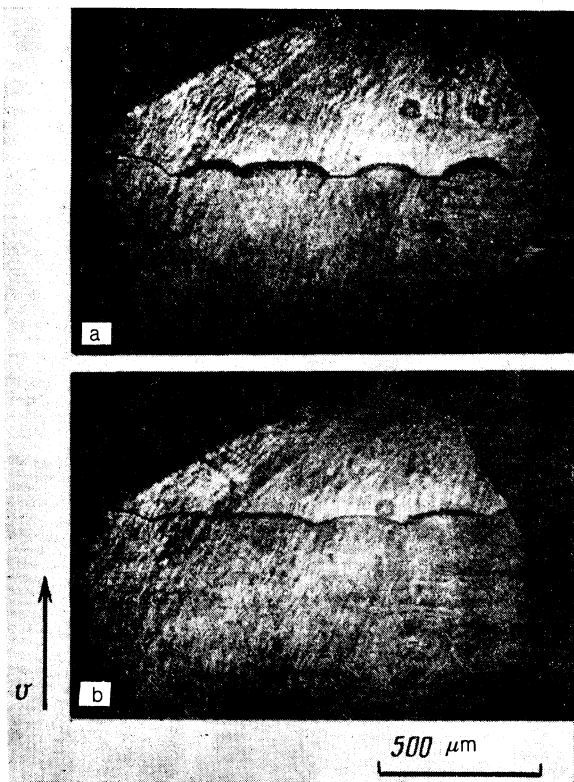


FIG. 4. Photographs of structures on a dynamic domain wall in YFeO_3 , obtained in the domain-wall contrast regime in a field $H = 1000$ Oe: a—3 ns after the start, b—15 ns after the start.

Figure 5 shows the time evolution of the structure. For the period $\lambda = 1200 \mu\text{m}$ the development time is 30 ns, after which the structure amplitude remains practically unchanged during the entire observation time. This time is substantially longer than the magnetic-subsystem relaxation time (on the order of 10^{-10} s), so that we can state with assurance that the periodic structure of the DW is quasistationary in magnetic fields that do not exceed greatly the field in which the motion becomes supersonic. In stronger fields, the structure development time is shorter. After reaching their maximum amplitudes, the structures relax nonlinearly. The ratio of their maximum amplitude to the period was 0.2 in all the investigated fields.

We have also performed an experiment in a different geometry. The controlling magnetic field was produced by a thin straight current-carrying conductor mounted parallel to the DW. Thus, the wall moved towards the wire in an increasing field. Periodic structures were produced on the moving DW in this case, too (Fig. 6). We point out that in such an experiment the wire and the DW must be very precisely parallel and the sample must be of very good quality.

4. THEORY

The equations describing the dynamics of the magnetization in a weak ferromagnet such as yttrium orthoferrite can be obtained from the following expressions for the Lagrangian L and the dissipation function R of the field $\mathbf{l}(r,t)$ (\mathbf{l} is the antiferromagnetism vector), see, e.g., Ref. 9 and 10-

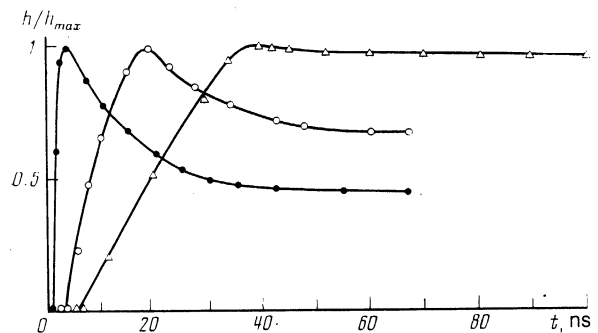


FIG. 5. Time dependence of the relative amplitude of the structures with different periods: ●— $\lambda = 260 \mu\text{m}$; ○— $\lambda = 500 \mu\text{m}$, △— $\lambda = 1200 \mu\text{m}$.

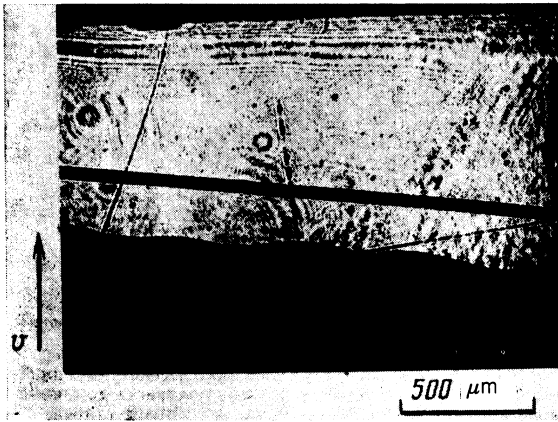


FIG. 6. High-speed photograph of the structure on a dynamic domain wall in the magnetic field of a thin straight current-carrying conductor.

$$L = \frac{1}{2} \left(\frac{M_0}{\gamma \omega_E} \right) \dot{\varphi}^2 - \frac{M_0}{\omega_E} \mathbf{H}_l \cdot [\dot{\varphi}] - E(\mathbf{l}, \nabla \mathbf{l}), \quad R = \alpha \frac{M_0}{2\gamma} \dot{\varphi}^2, \quad (1)$$

where γ is the gyromagnetic ratio, M_0 the sublattice magnetization, $\omega_E = \gamma A / 2M_0$, A the inhomogeneous-exchange constant (the exchange rigidity), $\mathbf{H}_l = \mathbf{H} + \mathbf{H}_D$, \mathbf{H}_D the Dzyaloshinskii field, α a dimensionless damping constant, and $E(\mathbf{l}, \nabla \mathbf{l})$ the system energy. In most cases the antiferromagnetism vector moves in a definite crystallographic plane, so that it can be defined using one angle variable. This is precisely how \mathbf{l} varies when the DW moves in yttrium orthoferrite, in which this plane is the ac plane of the crystal. In this case $l_x = \cos \varphi$, $l_y = 0$, $l_z = \sin \varphi$. The Lagrange and Rayleigh functions are then

$$L = \frac{1}{2} \frac{M_0}{\gamma \omega_E} \dot{\varphi}^2 - \frac{A}{2} (\nabla \varphi)^2 - K \sin^2 \varphi + M_s H \cos \varphi, \quad (2)$$

$$R = \alpha \frac{M_0}{2\gamma} \dot{\varphi}^2,$$

where K is the anisotropy constant in the (ac) plane and M_s is the saturation magnetization.

The DW is described by a soliton-type solution of the Lagrange-Euler equations corresponding to (2).^{11,12} We shall use an abbreviated description of such a soliton, wherein the DW is regarded as a two-dimensional surface (membrane) separating regions magnetized parallel and antiparallel to the field. This surface is specified by the equation $q = q(x, z, t)$, where q is the coordinate of the DW center. We assume that when the DW is at rest it is parallel to the $y = 0$ plane. The equation for $q(\mathbf{r}_1, t)$ can be obtained as the equation for slow variation of the adiabatic invariant of the field $\varphi(\mathbf{r}_1, t)$, i.e., the action, which has in this case the meaning of the system momentum. The adiabatic invariant can be defined as follows (see, e.g., Refs. 13 and 14):

$$P = \int_0^\pi \mathcal{P} d\varphi = - \int_{-\infty}^{+\infty} \frac{\partial L}{\partial \dot{\varphi}} \frac{\partial \varphi}{\partial \xi} d\xi, \quad (3)$$

where \mathcal{P} is the density of the wave pulse, $\xi = y - q(\mathbf{r}_1, t)$ the fast variable, and q varies slowly with t and \mathbf{r}_1 . At $H = 0$ and $\alpha = 0$ the distribution of the angle $\varphi(\mathbf{r}_1, t)$ is defined by the equation

$$\frac{\partial \varphi}{\partial \xi} = \frac{1}{\Delta(\dot{q}, \nabla_\perp q)} \sin \varphi,$$

$$\Delta(\dot{q}, \nabla_\perp q) = \Delta_0 [1 + (\nabla_\perp q)^2 - \dot{q}^2/c^2]^{1/2},$$

$$\Delta_0 = (A/K)^{1/2}, \quad \nabla_\perp = (\partial/\partial x, \partial/\partial z). \quad (4)$$

Substituting (4) in (3), we get

$$P = m_0 \dot{q} / [1 + (\nabla_\perp q)^2 - \dot{q}^2/c^2]^{1/2}, \quad (5)$$

where $m_0 = \sigma_0/c^2$ and $\sigma_0 = 4(AK)^{1/2}$ are the DW "rest mass" and energy density, and c is the maximum DW velocity.

The conservation equation for the action density is

$$\frac{\partial \mathcal{P}}{\partial t} - \text{div } \Pi = \frac{\partial L}{\partial y} + \frac{\partial R}{\partial \dot{\varphi}} \varphi_v',$$

where the action flux density Π is

$$\Pi_{x,z} = [\partial L / \partial (\varphi_{x,z'})] \varphi_v', \quad \Pi_y = (\partial L / \partial \varphi_v') \varphi_v' - L.$$

Substituting (3) in this equation and integrating with respect to the fast variable, we get

$$\frac{\partial P}{\partial t} + \frac{P}{\tau} - \nabla_\perp \sigma \nabla_\perp q = 2M_s H, \quad (6)$$

where

$$\tau^{-1} = \alpha \omega_E, \quad \sigma = \sigma_0 [1 + (\nabla_\perp q)^2 - \dot{q}^2/c^2]^{-1/2},$$

and P is defined by (5).

If the DW velocity is close to that of sound, account must be taken of the resonant interaction of the magnetic and elastic subsystems of the crystal, and this leads to the appearance of an additional retarding force $F_{me}(\dot{q}/[1 + (\nabla_\perp q)^2 - \dot{q}^2/c^2]^{1/2})$ (Refs. 7 and 8). Taking this into account, Eq. (6) becomes

$$\frac{\partial}{\partial t} \frac{m_0 \dot{q}}{[1 + (\nabla_\perp q)^2 - \dot{q}^2/c^2]^{1/2}} - \nabla_\perp \frac{m_0 c^2 \nabla_\perp q}{[1 + (\nabla_\perp q)^2 - \dot{q}^2/c^2]^{1/2}} + \frac{m_0 \dot{q}}{\tau [1 + (\nabla_\perp q)^2 - \dot{q}^2/c^2]^{1/2}} = 2M_s H + F_{me} \left(\frac{\dot{q}}{[1 + (\nabla_\perp q)^2 - \dot{q}^2/c^2]^{1/2}} \right). \quad (7)$$

We seek a particular solution of (7) in the form $q = vt + X(x)$. We change over in the equation for $X(x)$ to new variables ψ and x' , where ψ is defined by the equation

$$\sin \psi = \frac{-\partial X / \partial x}{[1 + (\partial X / \partial x)^2 - v^2/c^2]^{1/2}}, \quad x' = \frac{x}{(1 - v^2/c^2)^{1/2}},$$

and $\psi(x')$ is the angle between the normal to the DW and its velocity. We obtain

$$\frac{\partial \sin \psi}{\partial x'} = \frac{\mu}{\tau c^2} [H - H(v \cos \psi)], \quad \mu = 2M_s \tau (1 - v^2/c^2)^{1/2} / m_0, \quad H(u) = u / \mu - F_{me}(u) / 2M_s, \quad (8)$$

where $H(u)$ is the inverse dependence of the velocity on the field for a planar DW (see Fig. 7).

The form of the solution of Eq. (8) varies with the ratio of the velocity (which is now a bifurcation parameter) to u^* (the root of the equation $H(u) = H$). At $v > u^*$ Eq. (8) has

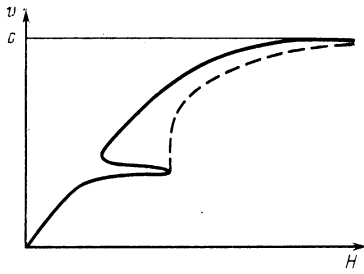


FIG. 7. Qualitative form of the velocity of a planar (solid curve) and a non-one-dimensional (dashed) DW as a function of the magnetic field.

no solutions bounded at infinity. At $v = u^*$ the solution is $\psi = 0$, corresponding to a planar DW. At $v < u^*$ Eq. (8) has periodic solutions. The phase portrait of the equation and the forms of the solutions are shown in Fig. 8. At the minima of the $X(x)$ curve, the derivative jumps from $-\infty$ to $+\infty$, corresponding to a singularity of the "cusp" type on the DW. In the vicinity of the singularity located at the point x_s the solution of Eq. (7) takes the form $X \sim [M_0(c^2 - v^2)|x - x_s|/M_s H]^{1/2}$. Integrating (8) and returning to the argument x , we obtain the period of the structure

$$\lambda = \left(1 - \frac{v^2}{c^2}\right)^{1/2} \frac{\tau c^2}{\mu} \int_{-\pi/2}^{\pi/2} \frac{\cos \psi d\psi}{H - H(v \cos \psi)}. \quad (9)$$

5. DISCUSSION OF RESULTS AND CONCLUSIONS

It can be seen from (9) that the period of the structure depends not only on the controlling field but also on the DW velocity. By varying v we can find the minimum permissible period $\lambda_{\min}(H)$ of the structure for a given field. At H^* corresponding to the right-hand edge of the region of constant velocity close to that of sound, $\lambda_{\min}(H)$ tends to infinity. With increase of field, $\lambda_{\min}(H)$ decreases rapidly (see Fig. 3). To ascertain which of the permissible λ is realized, we must consider the near-sonic flexural instability that causes a moving planar DW to become non-one-dimensional. As shown in Ref. 3, for a DW to be stable it is necessary to meet at all values of the wave vector k , the condition

$$B(k, H_z') < 0, \quad (10)$$

where

$$B(k, H_z') = 16M_s^2 h^{-1} [\ln(kh/2) + \gamma_E + K_0(kh)] - \sigma_0 k^2 - 2M_s H_z',$$

$K_0(kh)$ is a modified Bessel function of order zero, h is the sample thickness, $\gamma_E = 0.5772$ is the Euler constant, and σ_0 is the DW surface-energy density.

Under the conditions of our experiment, the gradient of H_z is larger than critical, i.e., the condition (10) is met, so that the immobile DW is flat. However, linearizing (7) with respect to the one-dimensional stationary solution with allowance for the magnetostatic interactions with the poles on the sample surface, and recognizing that $v^2/s^2 \ll 1$ near the speed of sound, we can show that if

$$\frac{\partial F_{me}}{\partial v} - \frac{2M_s}{\mu_0} > 2[m_0 |\max B(k, H_z')|]^{1/2} \quad (11)$$

($\mu_0 = 2M_s \tau / m_0$ is the initial mobility) and the condition (10) is met, a planar DW is flexurally unstable and the largest growth rate is possessed by the mode with the wave vector k^* corresponding to the maximum of $B(k, H_z')$. Condition (11) can be met only on sections with negative differential mobility at sufficiently high initial mobility μ_0 . A numerical search for the maximum of the function $B(k, H_z')$, carried out at $h = 100 \mu\text{m}$, $M_s = 8 \text{ G}$, and $m_0 = 2 \cdot 10^{-13} \text{ g/cm}$, yielded $\lambda = 2\pi/k^* = 250 \mu\text{m}$. The condition $\lambda \geq \lambda_{\min}$ under which the period λ is admissible is met all the way to the vicinity of the right-hand edge of the sound field H^* . As the field approaches H^* , by virtue of the growth of $\lambda_{\min}(H)$, the period λ should increase and should become infinite at $H = H^*$, in agreement with the experimental results. It can be seen from (9) that the $v(H)$ dependence for a periodic DW, i.e., for a finite λ , differs from the field dependence of the velocity for a planar wall (see Fig. 7).

Numerical estimates show that in supersonic motion of a DW the magnetostatic interaction is negligibly small compared with the terms contained in Eq. (7), and does not influence the form of the produced structure. It need therefore be taken into account only in the region of unstable

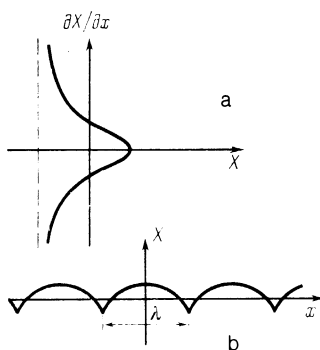


FIG. 8. a) Phase portrait of the equation describing singular dissipative structures on a dynamic domain wall. b) Qualitative form of stationary periodic solution of Eq. (8).

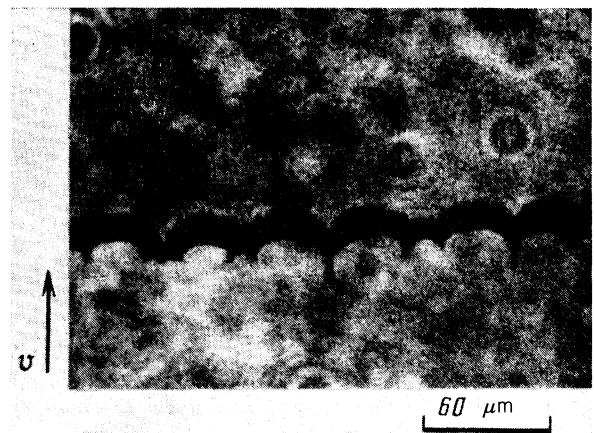


FIG. 9. Twofold high-speed photograph of the structure on a dynamic domain wall of an iron-garnet film with perpendicular anisotropy, in a field $H = 70 \text{ Oe}$ and for a delay $\Delta t = 0.4 \mu\text{s}$ between the light pulses.

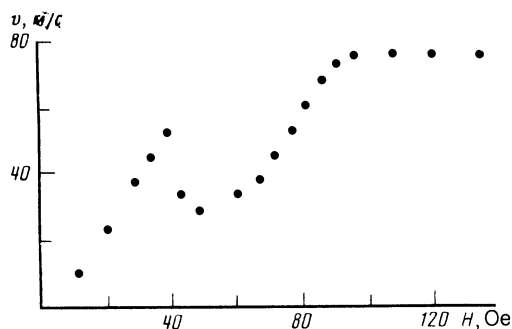


FIG. 10. Domain-wall velocity vs the magnetic field in an iron-garnet film.

motion, to eliminate the uncertainty introduced by Eq. (7) in the values of the structure period, as was indeed done here. As seen from Eq. (7), the equilibrium form of a stationary moving DW is determined by the balance of forces of three types: surface tension forces, pressure forces exerted by the external field, and deceleration forces due to dissipation in the magnetic and elastic subsystems. This corroborates the proposed dissipative mechanism of formation of periodic structures on a dynamic DW. The magnetostatic interaction apparently determines the period of the structures on the DW in magnetic fields substantially stronger than in the right-hand edge of the region of constant velocity (see Fig. 3). It is probable that the dissipative mechanism of structure formation on DW is typical not only of weak ferromagnets.

One more example of a structure of this type is shown in Fig. 9. Such a structure is realized in a $(\text{BiLaTm})_3(\text{FeGa})_5\text{O}_{12}$ film with easy magnetization axis perpendicular to the film plane. It occurs in the region $H > H_c$ after passage through the Slonczewski peak velocity.¹⁵ The cause of the instability of the planar DW front is here apparently the presence, just as in the orthoferrite case, of a negative differential mobility on the $v(H)$ plot (Fig. 10). Note the existence of singular "cusp" points on the DW, where vertical Bloch lines accumulate. It appears that the first results of observation of the structures on the dynamic DW of iron-

garnet films were published in Ref. 16, where they were observed, however, at above-limit velocities. No singularities were observed in this case on the dynamic DW.

We have shown in this paper, experimentally and theoretically, with orthoferrite and iron-garnet films as examples, that dissipative structures are produced on a moving DW. A remarkable feature of these structures is the presence of singularities where the derivatives of the displacements become discontinuous.

The onset of dissipative structures in the considered materials is due to the presence of a region of negative differential mobility on the plot of the DW velocity vs the magnetic field. It seems to us that the concept of magnetic dissipative structures is important for further development of ferromagnetodynamics.

The authors thank A. M. Balbashov for supplying the orthoferrite single crystals.

¹M. V. Chetkin and A. de la Campa, *Pis'ma Zh. Eksp. Teor. Fiz.* **27**, 168 (1978) [*JETP Lett.* **27**, 157 (1978)].

²H. Haken, *Synergetics*, Springer, 1978 (pp. 42 and 313 in Russ. transl.).

³F. B. Hagedorn, *J. Appl. Phys.* **41**, 1161 (1970).

⁴M. V. Chetkin, S. N. Gadeskiĭ, *et al.*, *Zh. Eksp. Teor. Fiz.* **86**, 1411 (1984) [*Sov. Phys. JETP* **59**, 825 (1984)].

⁵M. V. Chetkin, S. N. Gadeskiĭ, and A. I. Akhutkina, *Pis'ma Zh. Eksp. Teor. Fiz.* **35**, 373 (1982) [*JETP Lett.* **35**, 459 (1982)].

⁶M. V. Chetkin, S. N. Gadetskiĭ, V. N. Filatov, *et al.*, *Zh. Eksp. Teor. Fiz.* **89**, 1445 (1985) [*Sov. Phys. JETP* **62**, 837 (1985)].

⁷V. G. Bar'yakhtar, B. A. Ivanov, and A. L. Sukstanskiĭ, *ibid.* **75**, 2183 (1978) [**48**, 1100 (1978)].

⁸A. K. Zvezdin, A. A. Mukhin, and A. F. Popkov, Preprint No. 108 FIAN SSSR, 1982.

⁹V. G. Bar'yakhtar, B. A. Ivanov, and A. L. Sukstanskiĭ, *Zh. Eksp. Teor. Fiz.* **78**, 1590 (1980) [*Sov. Phys. JETP* **49**, 757 (1980)].

¹⁰A. F. Andreev and V. I. Marchenko, *Usp. Fiz. Nauk* **130**, 39 (1980) [*Sov. Phys. Usp.* **23**, 21 (1980)].

¹¹A. K. Zvezdin, *Pis'ma Zh. Eksp. Teor. Fiz.* **29**, 605 (1979) [*JETP Lett.* **29**, 553 (1979)].

¹²V. T. Bar'yakhtar, B. A. Ivanov, and A. L. Sukstanskiĭ, *Pis'ma v ZhTF* **4**, 853 (1979) [*Sov. Phys. Tech. Phys. Lett.* **4**, 344 (1979)]. *Zh. Eksp. Teor. Fiz.* **78**, 1509 (1980) [*Sov. Phys. JETP* **51**, 757 (1980)].

¹³G. B. Witham, *Linear and Nonlinear Waves*. Wiley, 1974 (p. 151 of Russ. transl.).

¹⁴W. D. Hayes, *Nonlinear Waves* [Russ. Transl.] Mir, 1977, p. 181.

¹⁵A. P. Malozemoff and J. C. Slonczewski, *Magnetic Domain Walls in Bubble Materials*, Academic, 1979 (p. 362 of Russ. transl.).

¹⁶V. G. Kleparsky *et al.*, *IEEE Trans. MAG-17*, 2775 (1981).

Translated by J. G. Adashko